Importance of the interband contribution to the magneto-refractive effect in Co/Cu multilayers

2003 J. Phys.: Condens. Matter 15 L695

(http://iopscience.iop.org/0953-8984/15/45/L02)

INSTITUTE OF PHYSICS PUBLISHING JOURNAL OF PHYSICS: CONDENSED MATTER

J. Phys.: Condens. Matter **15** (2003) L695–L702 PII: S0953-8984(03)69955-8

LETTER TO THE EDITOR

Importance of the interband contribution to the magneto-refractive effect in Co/Cu multilayers

R J Baxter[1], D G Pettifor[1], E Y Tsymbal[2], D Bozec[3], J A D Matthew[3] and S M Thompson[3]

[1] Department of Materials, University of Oxford, Parks Road, Oxford OX1 3PH, UK
[2] Department of Physics and Astronomy, University of Nebraska, Lincoln, NE 68588, USA
[3] Department of Physics, University of York, Heslington, York YO10 5DD, UK

Received 6 October 2003
Published 31 October 2003
Online at stacks.iop.org/JPhysCM/15/L695

Abstract

The optical properties of Co/Cu multilayers are investigated theoretically using a multiband tight-binding model and the results are compared to experimental data on the magneto-refractive effect (MRE). The optical conductivity of both parallel and antiparallel configurations of Co/Cu multilayers is calculated using the Kubo–Greenwood formula. The Kramers–Kronig relations are utilized to obtain the imaginary part of the conductivity and the real part of the dielectric function. The conductivity is decomposed into the intraband and interband terms, so that their different contributions to the MRE may be analysed. In particular, we find that the competition between the intraband and interband contributions leads to a change of sign in the MRE as a function of frequency, a feature which is also observed experimentally in the infrared region. This is in contrast to the predictions of the Drude model, where only the intraband part of the conductivity is considered and the MRE curve always takes the same sign. Therefore, it is vital to include the interband contribution for a full spectral study of the origin of the infrared MRE data.

1. Introduction

The relatively recent surge in interest in giant magneto-resistance (GMR) [1, 2] has been due to the wealth of possible applications in the data storage industry, as well as its general scientific interpretation. GMR is the result of the change in electrical resistance due to an applied magnetic field. In a multilayered system, composed of alternating layers of magnetic and non-magnetic materials, the resistance depends on whether the magnetic layers are aligned parallel or antiparallel due to spin-dependent scattering [3, 4]. The change in the conductivity between the parallel and antiparallel configurations also causes a change in the reflectivity; in the infrared spectral region this is called the magneto-refractive effect (MRE) [5]. As conventional measurements of GMR utilize contacts which are capable of damaging the surface, it is

of practical interest to have a contactless way of probing the magnitude of the GMR. The MRE, which has been measured in multilayers and granular films [5–8], has the potential of providing such a way [9, 10]. In fact, it has been reported that in the low frequency regime the MRE is closely related to the GMR [8–10]. Although the GMR effect has been investigated theoretically in many papers (e.g. [11–16]), to the best of our knowledge a theoretical analysis of the MRE is still lacking.

In this letter, we model the MRE and provide a deeper understanding of its major features as seen experimentally. In section 2, we present the computational and experimental details. In section 3, the theoretical results for Co/Cu multilayers are presented and compared with results obtained by other computational methods and by experiment. The conductivity, reflectivity and MRE are discussed and, in particular, the relative contributions of the intraband and interband contributions to the conductivity are considered along with their corresponding effects on the MRE. This allows us to investigate the traditional Drude model, where only intraband transitions are considered. In section 4 we conclude that the inclusion of the interband contribution is vital when investigating the MRE.

2. Methodology

The electronic structure of the Co/Cu multilayers is calculated using an orthogonal tight-binding (TB) approximation. The s, p and d valence orbitals are characterized by different on-site energy levels and the hopping integrals take the two-centre Slater–Koster form [12, 17]. These TB parameters are fitted to the *ab initio* band structures of the elemental metals [18]. The Co–Cu bond integrals were taken as the geometric mean of the Co–Co and Cu–Cu bond integrals. The band structure was calculated for both the parallel and antiparallel magnetizations of the Co_n/Cu_m multilayer for different values of n and m. In the parallel case, the unit cell consisted of n layers of Co and m of Cu, whereas the antiparallel case required double these amounts in order to account for the two different magnetization directions.

The spin conductivity, $\sigma^{\mu\nu}(\omega)$, at angular frequency ω is then calculated using the Kubo–Greenwood formula [19, 20]:

$$\operatorname{Re}\sigma^{\mu\nu}(\omega) = \frac{e^2}{\Omega\omega\pi}\int \mathrm{d}k \sum_{n,m}\int_{E_\mathrm{f}-\hbar\omega}^{E_\mathrm{f}} \operatorname{Im}\frac{1}{E - E_n + \mathrm{i}\gamma} v_{nm}^{\mu} \operatorname{Im}\frac{1}{E - E_m + \hbar\omega + \mathrm{i}\gamma} v_{mn}^{\nu}\,\mathrm{d}E \tag{1}$$

where Ω is the volume of the unit cell, E_m and E_n are the eigenvalues corresponding to bands m and n, respectively, and E_f is the Fermi energy. The matrix elements of the velocity operator, v_{nm}^{μ}, are calculated using $\hbar v^{\mu}(\mathbf{k}) = \partial H^0(\mathbf{k})/\partial k^{\mu}$, where H^0 is the single-particle Hamiltonian of the multilayer, $\mathbf{k}$ is the wavevector and μ is a Cartesian component. In equation (1) for simplicity we assume that the scattering operator is represented by the spin- and state-independent scattering parameter γ. Although this approximation leads to reduced values of GMR, it preserves the main features of the MRE discussed below and makes our calculations much less complicated, since it allows us to perform the integral in equation (1) analytically. The conductivity is calculated for parallel and antiparallel configurations for the Co/Cu multilayers, assuming that the up-spin and down-spin electrons are independent, as in the Mott model [21, 22].

The dielectric function is obtained from the relation $\varepsilon(\omega) = 1 + 4\pi\mathrm{i}\sigma/\omega$, in which the real and imaginary parts of the dielectric function are related to the imaginary and real parts of the conductivity, respectively. The real part of the dielectric function is evaluated from the

Kramers–Kronig formula:

$$\mathrm{Re}\,\varepsilon(\omega) = \frac{2}{\pi}\int_0^\infty \frac{\omega'\,\mathrm{Im}\,\varepsilon(\omega')\,\mathrm{d}\omega'}{\omega'^2-\omega^2}. \tag{2}$$

The reflectivity for p-polarized light follows from the relation

$$R = |(N\cos\theta - \cos\phi)/(N\cos\theta + \cos\phi)|^2, \tag{3}$$

where N is the complex refractive index, θ is the angle of incidence and ϕ is the complex angle of refraction in the medium, given by $\cos\phi = \sqrt{1-\sin^2\theta/N^2}$. Finally, the MRE is obtained by finding the percentage change in reflectivity between the antiparallel and parallel configurations, namely

$$\mathrm{MRE}\ (\%) = \frac{R_{\mathrm{AP}} - R_{\mathrm{P}}}{R_{\mathrm{P}}} \times 100 = \frac{\Delta R}{R}\ (\%). \tag{4}$$

The experimental measurements were made on an antiferromagnetically coupled Co/Cu multilayer prepared by sputtering at the University of Leeds. The structure of the film deposited onto a silicon substrate was Cr(105 Å)/[($\mathrm{Co}_{15.5\,\text{Å}}$/$\mathrm{Cu}_{7\,\text{Å}}$)]$_{25}$. MRE measurements were performed using a Nicolet Fourier transform infrared reflection spectrometer with a resolution better than 0.25 μm and a liquid nitrogen-cooled HgCdTe detector. Room temperature spectra were collected between 2.5 and 20 μm in a maximum applied magnetic field of +13.3 kOe. The MRE was obtained for p-polarized light using a KRS-5 grid polarizer and for an incidence angle of 65° with respect to the surface normal. The sample was further magnetically characterized at room temperature using a vibrating sample magnetometer and electrical current in-plane DC magnetotransport measurements were made using a four-point probe with a 1 mA applied current in a maximum applied magnetic field of ±9 kOe.

3. Results and discussion

Figure 1(a) shows the real part of the conductivity, which has been calculated for various different Co/Cu multilayer compositions. Bulk Co and bulk Cu are also included for comparison. The value of the scattering parameter, γ, in all these calculations was 0.1 eV. In bulk Cu, there is a peak at around 2 eV, which is attributed to the onset of interband transitions, in particular the contribution to the optical conductivity of the d band, which lies around 2 eV below the Fermi level in bulk Cu. It should be noted that this feature is enhanced and the shoulder of the peak becomes more prominent when a smaller broadening than 0.1 eV is used in the calculations. A broader peak also exists for Cu just below 5 eV, which is also due to the interband contribution, as the intraband contribution in this region is minimal. Bulk Co, like Cu, shows a strong increase in Re σ for frequencies less than 0.5 eV, which is often referred to as the Drude peak as it is mainly dominated by intraband transitions. However, we will see later that the interband contribution, even in this low frequency regime, should not be neglected when discussing the MRE. There are further peaks in the bulk Co curve in the region of 2 eV and also a broader peak, rising before 5 eV. As expected, the multilayer results sit between those of bulk Cu and bulk Co. These theoretical results agree with the experimental data of Uba *et al* [23], where the real and imaginary parts of the conductivity were obtained from ellipsometric measurements for Co/Cu multilayers, bulk Co and bulk Cu. Our TB results also agree with the more sophisticated calculations which use the self-consistent spin-polarized fully relativistic linear muffin-tin orbital method within the local spin density approximation [23].

Figure 1(b) shows the imaginary part of the conductivity for the same systems. In order to facilitate direct comparison with the experimental curves given in [23], we have plotted the

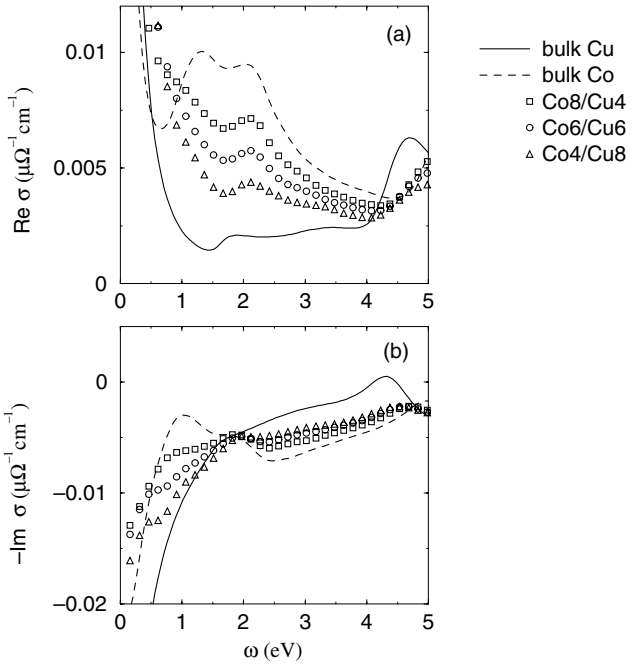

Figure 1. Frequency-dependent conductivity of different Co/Cu multilayers, bulk Co and bulk Cu, where (a) depicts the real part and (b) the imaginary.

negative of Im σ against ω. We find that good agreement is obtained with experiment. The Cu curve rises rapidly and then levels off at around 2 eV, where it crosses the Co curve. They then both rise with similar gradients between around 2.5 and 4 eV, before crossing over again around 5 eV.

In figures 2(a) and (b), the real part of the conductivities of the parallel and antiparallel configurations are plotted as a function of ω for the Co_8/Cu_4 multilayer. The individual intraband and interband contributions are also shown. In figure 2(c) the difference between the parallel and antiparallel conductivities is presented. The results are plotted for two different values of the scattering parameter, γ, namely 0.1 and 0.05 eV, where the corresponding values of GMR are 10% and 15%, respectively. As γ is varied, it is clear that the general trends between the right- and left-hand panels of the figure do not change. However, the features of the plot are accentuated and become more pronounced by using the smaller value of γ. This is particularly reflected in the narrowing of the intraband Drude peak as γ decreases due to its Lorentzian behaviour: the frequency-dependent conductivity $\sigma(\omega) = \sigma_0/(1 + \omega^2\tau^2)$, where σ_0 is the zero-frequency conductivity, ω is the frequency and τ is the relaxation time, related to γ by $1/\tau = 2\gamma$.

We see from figure 2(a) that, at zero frequency, the parallel-aligned multilayer shows a higher dc conductivity than the antiparallel-aligned multilayer, which reflects the GMR effect. Note that, due to our assumption of spin-independent scattering, the origin of GMR is entirely related to the difference in the electronic structure between the parallel and antiparallel configurations of the multilayer. The inset in figure 2(a) shows the contributions to the conductivity from the up- and down-spin electrons for the parallel configuration. We see that the up-spin channel possesses a higher conductivity than that of the down-spin; in the antiparallel case, both spin channels have equal conductivities which are similar to the latter. Importantly,

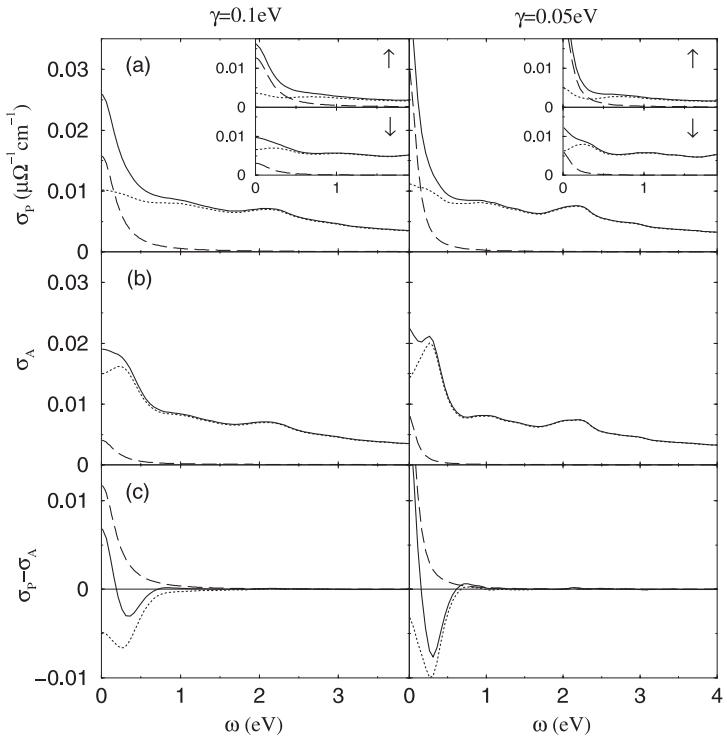

Figure 2. (a) Frequency-dependent conductivity of Co_8/Cu_4 for the parallel configuration. (b) As in (a) for the antiparallel configuration. (c) Difference in conductivity between the parallel and antiparallel configurations. The total (full curve), intraband (broken curve) and interband (dotted curve) contributions are shown. The inset shows the separate up-spin and down-spin conductivities for the parallel configuration. In the left-hand panel, the scattering parameter is 0.1 eV and 0.05 eV in the right-hand panel.

we observe that the low frequency conductivity of the up-spin electrons is dominated by the intraband contribution, due to the density of states around the Fermi level being sp and nearly free-electron-like, leading to Drude intraband transitions. In contrast, the interband contribution is more important for the down-spin conductivity due to the many d states in the vicinity of the Fermi level. In addition, the sp band hybridizes strongly with the d band, thereby reducing the Drude intraband contribution to the down-spin conductivity.

Figure 2(c) highlights the individual roles played by the intraband and interband contributions. It is clear that the difference in the intraband, or Drude, conductivity between the parallel and antiparallel configurations is always positive. In contrast, this difference remains negative for the interband contribution. The crucial point is that it is only when both intraband and interband contributions are considered together that a change of sign appears in $(\sigma_{\mathrm{P}} - \sigma_{\mathrm{A}})$ at 0.22 eV. As we will see later, this competition between these two contributions also leads to a change of sign in the MRE, a feature which is observed experimentally. Importantly, this result could not be obtained using the Drude model, as consideration of only intraband transitions would not lead to a change of sign in $(\sigma_{\mathrm{P}} - \sigma_{\mathrm{A}})$.

In figure 3 the reflectivity of the Co_8/Cu_4 multilayer is plotted for both parallel (full curve) and antiparallel (broken curve) configurations. The value of the scattering parameter, γ, is 0.1 eV. Both curves display quite similar trends; tending to 1 as ω tends to zero and generally

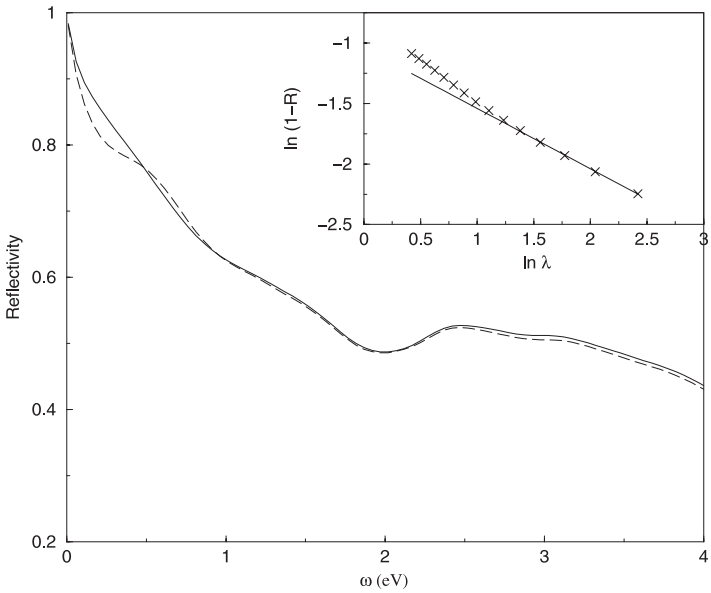

Figure 3. Reflectivity as a function of ω for parallel (full curve) and antiparallel (broken curve) configurations of Co_8/Cu_4. The inset displays $\ln(1 - R)$ against $\ln\lambda$ in the low energy regime. The data points from our calculations are depicted as crosses and the full line has a gradient of $-\frac{1}{2}$.

decreasing as ω increases, with some variations. In the low frequency regime, the conductivity of metals is relatively high, so that $\mathrm{Re}\,\sigma \gg \mathrm{Im}\,\sigma$. This leads to the imaginary part of the dielectric constant becoming much greater than the real part in this region and hence the metal is strongly reflecting. As ω increases from 0 to 0.45 eV the most striking difference between the configurations becomes apparent. The antiparallel reflectivity decreases much more rapidly than the parallel one, which can be understood as follows. In the low frequency regime, the real part of the optical conductivity is greater for the parallel configuration than the antiparallel one, as has been discussed above. This leads to the imaginary part of the dielectric constant assuming a larger value for the parallel configuration in this frequency regime, which means that the multilayer is more strongly reflecting. However, with increasing ω, we saw earlier that the conductivity becomes greater for the antiparallel configuration, before the difference in the configurations becomes relatively small. This behaviour is also featured in the reflectivity curves, as there is a crossover at around 0.5 eV when the antiparallel system becomes more strongly reflecting than the parallel. With increasing ω, the differences become much less pronounced.

In the low frequency regime, the Hagen–Rubens relation [24] should apply, where the reflectivity, R, is related to ω by

$$R \approx 1 - 2(\omega/2\pi\sigma)^{1/2} \tag{5}$$

for $\sigma \gg \omega$. This relation is valid in the low frequency or high wavelength regime. It implies that $(1 - R)$ should be directly proportional to $\lambda^{-1/2}$. The inset in figure 3 plots $\ln(1 - R)$ against $\ln\lambda$, where the crosses are the data points from our calculations and the full line has a gradient of $-\frac{1}{2}$. Our results are therefore consistent with the Hagen–Rubens relation at higher wavelengths, as expected.

In figure 4 the variation in the MRE with respect to frequency (or photon energy) is shown. Three different theoretical curves are plotted, each corresponding to a different value of the

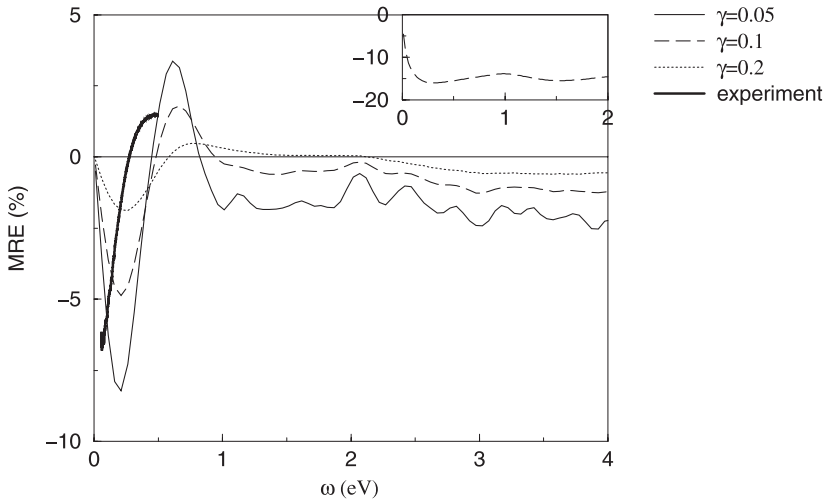

Figure 4. The MRE as a function of ω, where $\gamma = 0.05$ eV (full curve), 0.1 eV (broken curve) and 0.2 eV (dotted curve). The thick full curve is the experimental data. In the inset only the intraband contribution has been considered.

scattering parameter, γ, namely 0.05, 0.1 and 0.2 eV, respectively. The corresponding values of GMR are 5% ($\gamma = 0.2$ eV), 10% ($\gamma = 0.1$ eV) and 15% ($\gamma = 0.05$ eV). These values are lower than the experimental value of 45%, due to the same scattering parameter being used for both parallel and antiparallel configurations. This leads to a reduction in the zero frequency GMR value, compared to our earlier more accurate spin-dependent scattering parameter results (see equation (16) of [12]). As discussed previously, varying the scattering parameter γ affects the features of the plot: increasing γ yields a smoother curve, while decreasing γ leads to the features of the graph becoming more pronounced, just as we observe in figure 4. However, the predicted trends in the MRE remain the same.

Let us consider, in particular, the broken curve corresponding to $\gamma = 0.1$ eV. The major features of this curve lie in the relatively low frequency regime: a distinct minimum around 0.2 eV, a crossover of the ω axis at 0.5 eV and a peak around 0.7 eV. At high energies, the values of the MRE remain roughly constant. The thick full curve is the experimental data [25], where the most striking feature is the change of sign just below 0.3 eV. This crossover of the ω axis, which is reproduced in our results, albeit at a higher frequency, would not appear at all in a Drude calculation. This is illustrated in the inset in figure 4, where only the intraband contributions have been plotted for $\gamma = 0.1$ eV. We see that the MRE no longer displays a change of sign. Hence, the crucial change of sign is the result of the competition between intraband and interband contributions, where the latter is important at these relatively low frequencies and may not be neglected when considering the MRE.

4. Conclusions

The MRE in Co/Cu multilayers is investigated using a realistic electronic band structure within a TB approach. Using the Kubo–Greenwood formula, the optical conductivity is calculated as a function of frequency for parallel and antiparallel magnetizations of the multilayers. A change in sign is found in the conductivity difference, an effect attributed to the key roles played by the intraband and interband contributions. This also gives rise to a change of sign in the MRE, a feature which is observed experimentally. This characteristic is absent when only

the intraband contributions are considered, which means that the Drude model is not capable of describing accurately the MRE over the full spectral range due to its neglect of interband transitions.

This work has been funded by the EPSRC and Seagate Technology Northern Ireland. The calculations were performed in the Materials Modelling Laboratory (MML), Department of Materials, University of Oxford. The sample was provided by Dr C Marrows, University of Leeds, UK. Professor R Atkinson is gratefully acknowledged for helpful correspondence. EYT thanks the MML for hospitality during his stay in Oxford, summer 2003.

References

[1] Baibich M N, Broto J M, Fert A, Nguyen Van Dau F, Petroff F, Etienne P, Creuset G, Freiederich A and Chazellas J 1988 *Phys. Rev. Lett.* **61** 2472
[2] Binash G, Grünberg P, Saurenbach F and Zinn W 1989 *Phys. Rev.* B **39** 4828
[3] Levy P M 1994 *Solid State Phys.* **47** 367
[4] Tsymbal E Y and Pettifor D G 2001 *Solid State Phys.* **56** 113
[5] Jacquet J C and Valet T 1995 *Magnetic Ultrathin films, Multilayers and Surfaces* ed E Marinero (Pittsburgh, PA: Materials Research Society) p 477
[6] Uran S, Grimsditch M, Fullerton E and Bader S D 1998 *Phys. Rev.* B **57** 2705
[7] Van Driel J, de Boer F R, Coehoorn R and Rietjens G H 1999 *Phys. Rev.* B **60** 6949
[8] Kravets V G, Bozec D, Matthew J A D, Thompson S M, Menard H, Horn A B and Kravets A F 2002 *Phys. Rev.* B **65** 054415
[9] Gester M, Schlapka A, Pickford R A, Thompson S M, Camplin J P, Eve J K and McCash E M 1999 *J. Appl. Phys.* **85** 5045
[10] Camplin J P, Thompson S M, Loraine D R, Pugh D I, Collingwood J, McCash E M and Horn A B 2000 *J. Appl. Phys.* **87** 4846
[11] Zhang S, Levy P M and Fert A 1992 *Phys. Rev.* B **45** 8689
[12] Tsymbal E Y and Pettifor D G 1996 *Phys. Rev.* B **54** 15314
[13] Villeret M, Mathon J, Muniz R B and d'Albuquerque e Castro J 1998 *Phys. Rev.* B **57** 3474
[14] Brown R H, Nicholson D M C, Butler W H, Zhang X-G, Shelton W A, Schulthess T C and MacLaren J M 1998 *Phys. Rev.* B **58** 11146
[15] Zahn P and Mertig I 2001 *Phys. Rev.* B **63** 104412
[16] Zhuravlev M Ye, Schepper W, Heitmann S, Vinzelberg H, Zahn P, Mertig I, Lutz H O, Vedyayev A V, Reiss G and Hütten A 2002 *Phys. Rev.* B **65** 144428
[17] Slater J C and Koster G F 1954 *Phys. Rev.* **94** 1498
[18] Papaconstantopoulos D A 1986 *Handbook of the Bandstructure of Elemental Solids* (New York: Plenum)
[19] Kubo R 1957 *J. Phys. Soc. Japan* **12** 570
[20] Greenwood D A 1958 *Proc. Phys. Soc. Lond.* **71** 585
[21] Mott N F 1936 *Proc. R. Soc.* **156** 368
[22] Mott N F 1964 *Adv. Phys.* **13** 325
[23] Uba S, Uba L, Perlov A Ya, Yaresko A N, Antonov V N and Gontarz R 1997 *J. Phys.: Condens. Matter* **9** 447
[24] Ziman J M 1964 *Principles of the Theory of Solids* (Cambridge: Cambridge University Press)
[25] Vopsaroiu M, Bozec D, Marrows C, Perez M, Matthew J A D and Thompson S M 2003 at press